

# Structural and electrical properties of yttrium-doped ceria ceramic composites

A. M. IONASCU, I. MERCIONIU<sup>a,\*</sup>, P. V. NOTINGHER, N. POPESCU-POGRION<sup>a</sup>

*University Politehnica of Bucharest, 060042, Romania;*

*<sup>a</sup>National Institute of Materials Physics, Magurele-Bucharest, 077125, Romania*

The attractive properties of Yttria doped ceria, particularly the structural and material properties, have led to vast research efforts to investigate and develop such materials. One of the main applications of this ceramic is in the IT-SOFC. The aim of this paper is the preparation and characterization of Y doped Ceria and low doped  $\alpha$ -Al<sub>2</sub>O<sub>3</sub>, a new composite for IT-SOFC (10 mol %) Y:CeO<sub>2</sub> and (150 ppm) Y: $\alpha$ -Al<sub>2</sub>O<sub>3</sub> composite were obtained by sol-gel or mechanical route for 10YDC and 150 Y: $\alpha$ -Al<sub>2</sub>O<sub>3</sub>. Shapes, size distributions and the mean of grains were determined by SEM, EDX and statistical investigations.

(Received June 2, 2011; accepted July 25, 2011)

*Keywords:* Ceramic composite, Y:CeO<sub>2</sub>, Y:Al<sub>2</sub>O<sub>3</sub>

## 1. Introduction

In the 20<sup>th</sup> century, fossil fuels were the main source of energy. Increasing energy demand, global warming, pollution, loss of natural fuel deposits, led to search for new sources of energy (cheaper and cleaner). In recent years to produce electricity, new technologies and equipments were developed. This new technology has been developed to produce electricity: photovoltaic batteries, aeolian turbines, geothermal heat pumps, nuclear fusion, fuel cells (solid electrolyte, polymer membrane, molten carbonate, etc.) [1, 2].

Fuel cells are constructed of two electrodes (anode, cathode) and an electrolyte [2]. The most common are the electrolyte polymer type (Polymer electrolyte Fuel Cell - PEMFC) and the one with ceramic oxides (Solid Oxide Fuel Cell - SOFC) [3]. Most of the problems which designers face regarding these cells are due to the choice of electrolyte, because the electrode design and the materials used in their production depend on the electrolyte [4].

The most commonly used SOFC electrolyte, which operates in the temperature range (900 – 1000 °C) is zirconium dioxide ZrO<sub>2</sub> stabilized with yttrium trioxide Y<sub>2</sub>O<sub>3</sub> (noted 10 YSZ) [5, 6]. To increase fuel cells lifetime, the temperature decrease, in operating range (600 - 650 °C) obtaining solid oxide for intermediate temperature fuel cell (IT-SOFC). The electrolyte of these cells must satisfy a number of conditions: the average particle diameter < 100 nm, average grain diameter < 1  $\mu$ m, less porosity, electrical and ionic conductivity as large as possible at the operating cell temperature ( $\sim 2.23 \times 10^{-3}$  S/cm at 600 °C) [2].

Structural, electrical and mechanical properties of IT-SOFC solid oxide electrolytes depend on the amount and type of dopant used. Thus, the YSZ electrolyte is not suitable for IT-SOFC because in the temperature range

(600-650 °C), ionic conductivity is relatively low. To increase the ionic conductivity values, a higher amount of dopant is required, but if the content of dopant is too high, it is unfavorable to the mechanical properties, which are reduced [7]. To eliminate these disadvantages, the following methods have been proposed: (i) replacement the classical doping yttrium (Y) with scandium (Sc) for zirconium dioxide (ZrO<sub>2</sub>), (ii) replacement the ZrO<sub>2</sub> with cerium dioxide (CeO<sub>2</sub>) and (iii) use of Y and Sc co-doping [8, 9].

Among the electrolytes used for IT-SOFC, the most studied are those based on CeO<sub>2</sub>. They are doped with yttrium trioxide (Y<sub>2</sub>O<sub>3</sub>), scandium trioxide (Sc<sub>2</sub>O<sub>3</sub>), Y<sub>2</sub>O<sub>3</sub> + Sc<sub>2</sub>O<sub>3</sub>, gadolinium (Gd), samaria (Sm), etc.

This paper presents a study on the morphological and electrical properties of a new ceramic composite used as solid electrolyte for IT-SOFC. This composite represented by the formula [(90 %) 10 Y<sub>2</sub>O<sub>3</sub>: CeO<sub>2</sub> + (10 %) (150 ppm) Y<sub>2</sub>O<sub>3</sub>:  $\alpha$  - Al<sub>2</sub>O<sub>3</sub>] is composed of (10 mol %) Y<sub>2</sub>O<sub>3</sub> doped CeO<sub>2</sub> (denoted 10 YDC) and (10 %) (150 ppm) Y<sub>2</sub>O<sub>3</sub> doped  $\alpha$  - Al<sub>2</sub>O<sub>3</sub> (denoted 150 Y :  $\alpha$  - Al<sub>2</sub>O<sub>3</sub>).

## 2. Experiments

### 2.1 Samples

For experiments, two types of ceramic composite samples 10 Y<sub>2</sub>O<sub>3</sub> : CeO<sub>2</sub> + (10 %) (150 ppm) Y<sub>2</sub>O<sub>3</sub> :  $\alpha$  - Al<sub>2</sub>O<sub>3</sub> were used, denoted by A and B.

Samples A were made, by mechanical mixing, of two commercial nanopowders (INFRAMAT - U.S.A): 10 YDC (90 %) and 150 Y<sub>2</sub>O<sub>3</sub> :  $\alpha$  - Al<sub>2</sub>O<sub>3</sub> (10 %).

Samples B were made by mechanical mixing of two nanopowders, 10 YDC (90 %) and 150 Y<sub>2</sub>O<sub>3</sub> :  $\alpha$  - Al<sub>2</sub>O<sub>3</sub> (10 %) both synthesized by sol-gel method.

The mixtures (for both samples A and B) were homogenized mechanically, compacted in a cylindrical

shape at 3000 kgf and sintered at 1500 °C for 2 h [10]. Both types of samples present a cylindrical shape with a diameter of 10 mm and a thickness of 1.2 mm.

## 2.2. Equipments

Morphological analyses (grain shape, average grain diameter, porosity) of the samples were performed by scanning electron microscopy (SEM). Qualitative elemental analysis (to determine the nature and distribution of chemical elements inside the samples) was made by energy dispersive X-ray spectroscopy (EDX). To obtain the SEM and EDX images, a scanning electron microscope type FEI Quanta Inspect F was used.

Measurements of the real  $\epsilon_r'$  and imaginary  $\epsilon_r''$  parts of the complex relative permittivity, the real  $\sigma'$  and imaginary  $\sigma''$  parts of the complex conductivity and loss factor  $\tan \delta$  were made with a NOVOCONTROL dielectric spectrometer. On the samples surfaces, a thin layer of silver (Ag) was deposited by vacuum evaporation.

$\epsilon_r'$ ,  $\epsilon_r''$ ,  $\sigma'$ ,  $\sigma''$  and  $\tan \delta$  measurements were performed at a  $1V_{rms}$  voltage, frequency  $f = 10^5$  Hz and temperatures 100, 200, 300, 400 °C.

## 3. Results and discussions

### A. Morphological characterization

A part of the results obtained by SEM for the two samples A and B are shown in Figs. 1 - 6.

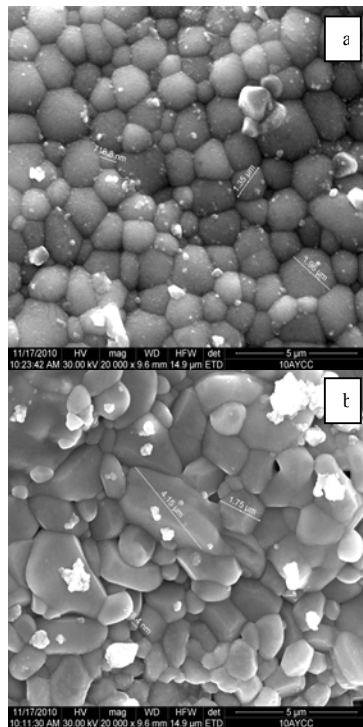


Fig. 1. Scanning electron microscopy for sample A (a) area 10 YDC, (b) area 150 Y:  $\alpha$ - $Al_2O_3$ .

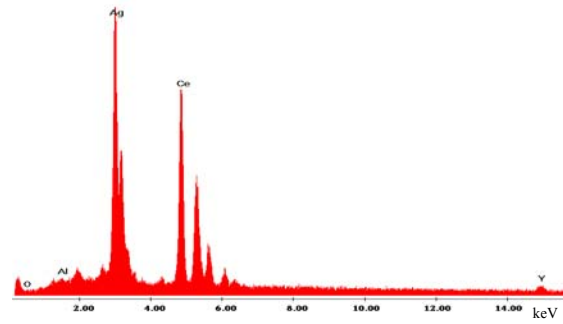


Fig. 2. EDX spectrum for the (a) areas of sample A.

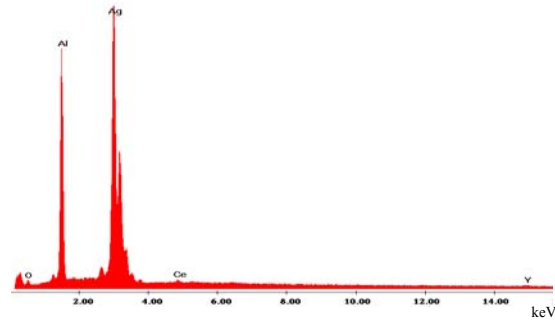


Fig. 3. EDX spectrum for the (b) areas of sample A.

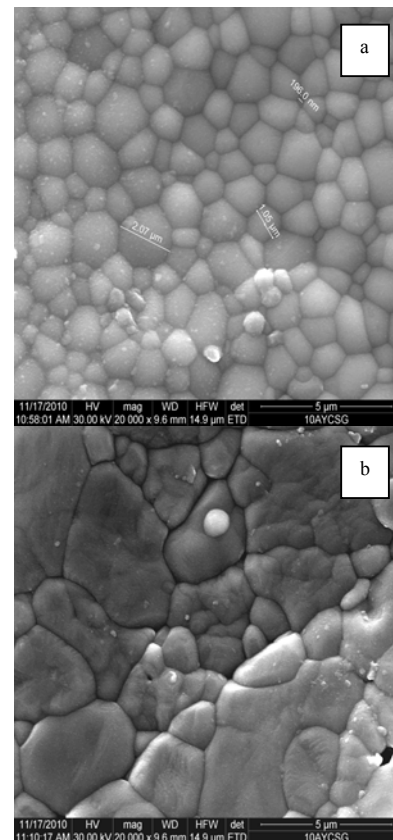


Fig. 4. Scanning electron microscopy for sample B (a) area 10 YDC, (b) area 150 Y:  $\alpha$ - $Al_2O_3$ .

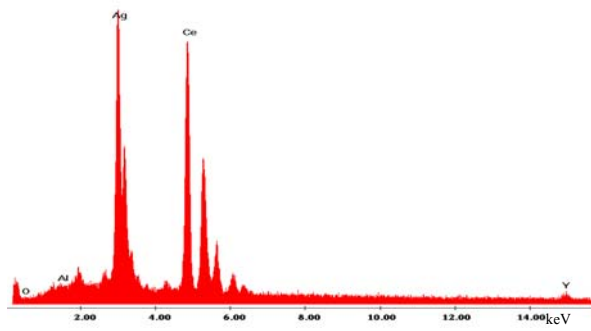


Fig. 5. EDX spectrum for the (a) areas of sample B.

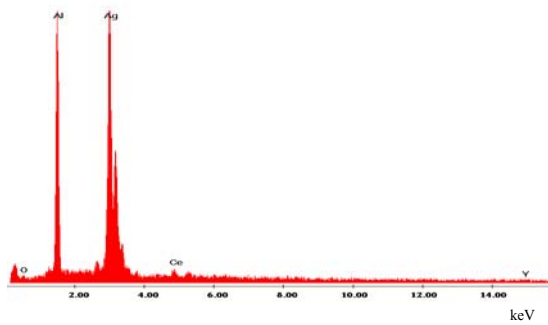


Fig. 6. EDX spectrum for the (b) areas of sample B.

## B. Electrical properties

The results obtained by measuring the real ( $\epsilon_r'$ ) and imaginary ( $\epsilon_r''$ ) parts of the relative permittivity, the real ( $\sigma'$ ) and imaginary ( $\sigma''$ ) parts of conductivity and loss factor ( $\tan \delta$ ) at temperatures 100, 200, 300 and 400 °C, for the two samples are presented in Figs. 7 - 12.

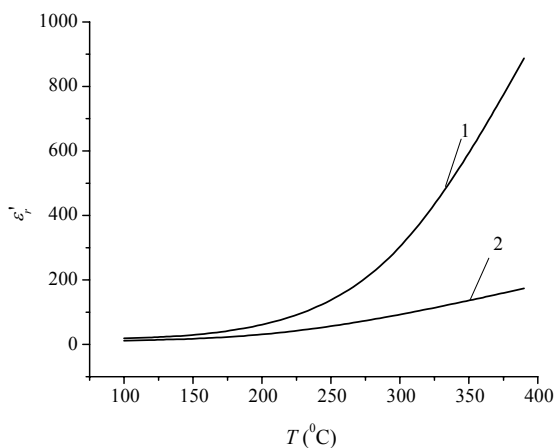


Fig. 7. Variation of the real component of complex permittivity ( $\epsilon_r'$ ) with temperature ( $T$ ) for samples A (1) and B (2).

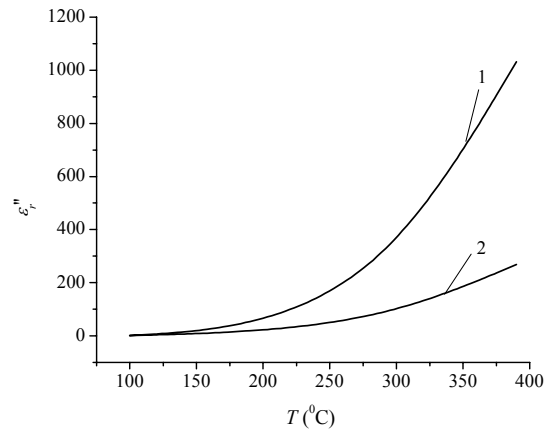


Fig. 8. Variation of the imaginary component of complex permittivity ( $\epsilon_r''$ ) with temperature ( $T$ ) for samples A (1) and B (2).

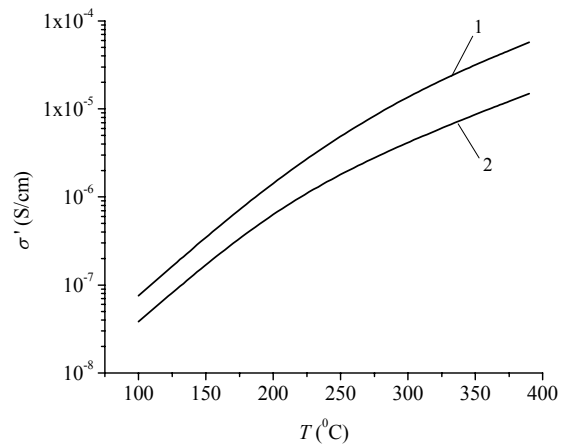


Fig. 9. Variation of the real component of complex conductivity ( $\sigma'$ ) with temperature ( $T$ ) for samples A (1) and B (2).

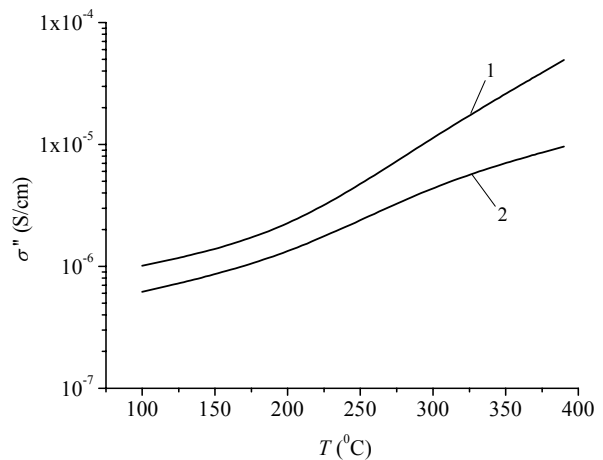


Fig. 10. Variation of the imaginary component of complex conductivity ( $\sigma''$ ) with temperature ( $T$ ) for samples A (1) and B (2).

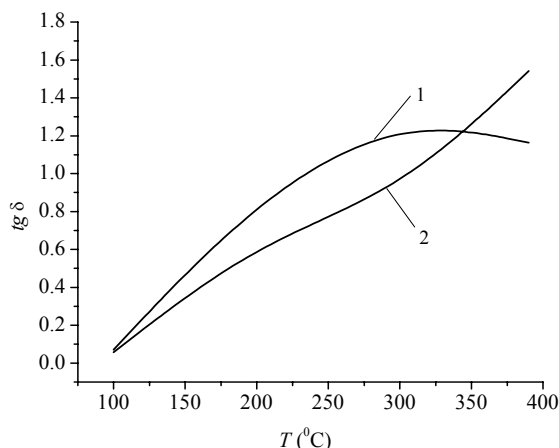


Fig. 11. Variation of loss factor ( $\text{tg } \delta$ ) with temperature ( $T$ ) for samples A (1) and B (2).

#### 4. Discussions

Fig. 1 shows the agglomerates of 10 YDC and of 150 Y:  $\alpha$ - $\text{Al}_2\text{O}_3$ , according to EDX analysis performed in areas (a) and (b). Following the morphological analysis performed on sample A, it was found the presence of polyhedral grains of  $\text{Y}_2\text{O}_3$  doped  $\alpha$ - $\text{Al}_2\text{O}_3$  without intragranular pores and few-intergranular pores (average grain diameter  $d_M = 0.0075 \pm 1.5 \mu\text{m}$ ). 10 YDC agglomerates are very compact, having grains with rounded edges, with an average diameter  $d_M = 0.065 \pm 1.36 \mu\text{m}$ . The compact agglomerates of 150 Y:  $\alpha$ - $\text{Al}_2\text{O}_3$  are uniformly distributed in the 10 YDC agglomerates.

Figs. 2 and 3 indicate the presence of cerium, yttrium, oxygen and silver, respectively aluminum, yttrium, oxygen and silver elements in (a, b) areas. The silver was deposited by evaporation on the sample surface, for metallization.

In Fig. 4 can be seen areas of 10 YDC and areas of 150 Y:  $\alpha$ - $\text{Al}_2\text{O}_3$ . In agglomerates of 150 Y:  $\alpha$ - $\text{Al}_2\text{O}_3$  are put in evidence grains with polyhedral shape, with an average diameter  $d_M = 0.012 \pm 1.88 \mu\text{m}$ , forming a dense mass with very low porosity,  $P < 0.2 \%$ . These agglomerates are uniformly distributed in the 10 YDC agglomerates. The agglomerates of 10 YDC show uniform grains of polyhedral shape with rounded edges and with average size  $d_M = 0.061 \pm 1.27 \mu\text{m}$  and a low porosity  $P < 2 \%$ . Porosity between composite components was about 4–5%.

EDX spectrum from Figs. 5 and 6 reports the presence of cerium, yttrium, oxygen and silver, respectively aluminum, yttrium, oxygen and silver. The silver was deposited by evaporation on the sample surface, for metallization.

The EDX spectra for samples A and B (the peaks being characteristic for elements of cerium, aluminum, oxygen, yttrium), prove that the chemical composition of the material was respected.

Morphological characteristics (porosity and grain diameter) and conductivity are similar to those presented in the literature [12].

The values of all physical quantities ( $\epsilon_r'$ ,  $\epsilon_r''$ ,  $\sigma'$ ,  $\sigma''$ ,  $\tan \delta$ ) increase with temperature. On the other hand, the differences between the variations of real and imaginary components for the relative complex permittivity of samples A and B are very high for temperature values above 150 °C. Thus, for temperature  $T = 400$  °C, the difference between the values of  $\epsilon_r'$  is 80 % and between values of  $\epsilon_r''$  is 73.9 %.

The values of real and imaginary components of complex conductivity (Figs. 9 and 10) also increase with temperature. Conductivity increase with temperature is due to the intensification of diffusion of ions which participate in conduction process, diffusion constant having the expression:

$$D = fa^2/6 \exp(-W/kT) \quad (1)$$

where  $f$  is the oscillation frequency of ions,  $a$  - network constant,  $W$  - barrier height by escalation of ions,  $k$  - Boltzmann constant,  $T$  - thermodynamic temperature [11]. For all temperature values in the domain 100 - 400 °C, it was noticed that the conductivities values are higher in samples A than in samples B.

#### 4. Conclusions

In this paper, the structural and electrical properties of two types of samples of a new solid electrolyte (based on  $\text{Y}_2\text{O}_3$  doped  $\text{CeO}_2$  and low  $\text{Y}_2\text{O}_3$  doped  $\alpha$ - $\text{Al}_2\text{O}_3$ ) for IT-SOFC were analyzed.

It was found that the sintered composite samples A (obtained from nanopowders synthesized by mechanical homogenization method) have better structural characteristics compared with sintered composite samples B (obtained from nanopowders synthesized by sol-gel method). These results were revealed by morphological investigations (realized by SEM) in correlation with the elemental analyses (realized by EDX).

Electrical conductivity is higher for sample A, showing from this point of view, that sample A is better than sample B.

The ceramic composite 10  $\text{Y}_2\text{O}_3$ :  $\text{CeO}_2$  + (10 %) (150 ppm)  $\text{Y}_2\text{O}_3$ :  $\alpha$ - $\text{Al}_2\text{O}_3$  in which the  $\alpha$ - $\text{Al}_2\text{O}_3$  percentage varies will be used in future studies.

#### Acknowledgment

The authors would like to thank Dr. Petru Nita for assistance in obtaining scanning electron microscopy images.

#### References

- [1] E. Ivers-Tiffe, A. Weber, D. Herbstrutt, Journal of the European Ceramic Society, **21**, 1805 (2001).

- [2] G. Pasciak, K. Prociow, W. Mielkarek, B. Gornicka, B. Mazurek, *Journal of the European Ceramic Society*, **21**, 1867 (2001).
- [3] A. Baker, K. A. Adamson, *American Ceramic Society Bulletin*, **85**, 23 (2006).
- [4] H. He, Y. Huang, J. Regal, M. Boaro, G. M. Vohs, R. J. Gorte, *J. Am. Ceram. Soc.* **87**, 331 (2004).
- [5] Yueh-Hsun Lee, Chih-Wei Kuo, I-Ming Hung, Kuan-Zong Fung, Moo-Chin Wang, *Journal of Non-Crystalline Solids*, **351**, 3709 (2005).
- [6] Christel Laberty-Robert, Florence Ansart, Simone Castillo, Guillaume Richard, *Solid State Sciences*, **4**, 1053 (2002).
- [7] M. Dudek, J. Molenda, *Materials Science-Poland*, **24**, 45 (2006).
- [8] V. V. Ivanov, V. R. Khrustov, Yu. A. Kotov, A. I. Medvedev, A. M. Murzakaev, S. N. Shkerin, A. V. Nikonov, *Journal of the European Ceramic Society*, **27**, 1041 (2007).
- [9] M. A. Gülgün, V. Putlayev, M. Rühle, *J. Am. Ceram. Soc.* **82**, 1849 (1999).
- [10] A. M. Vlaicu, I. Mercioniu, B. S. Vasile, C. C. Negrila, C. Logofatu, N. C. Cretu, P. Nita, N. Popescu-Pogrion, *Optoelectron. Adv. Mater.-Rapid Commun.* **5**, 143 (2011).
- [11] P. V. Notingher, *Materials for electrotehnics*, Politehnica Press, Bucharest, **1**(32) 180 (2005).
- [12] A. Moure, J. Tartaj, C. Moure, *Journal of the European Ceramic Society*, **29**, 2559 (2009).

---

\*Corresponding author: imercioniu@infim.ro